Ab Initio Calculations and Display of Enantiomeric and Nonenantiomeric Anisotropic Circular Dichroism: The Lowest $\pi \rightarrow \pi^*$ Excitation in Butadiene, Cyclohexadiene, and Methyl-Substituted Cyclohexadienes†

Aage E. Hansen*

Department of Chemistry, H.C. Ørsted Institute, Universitetsparken 5,DK-2100 Copenhagen Ø, Denmark

Keld L. Bak

UNI-C, Olof Palmes Allé 38, DK-8200 Aarhus N, Denmark

Received: May 23, 2000; In Final Form: September 18, 2000

The relationship between anisotropic electronic circular dichroism (CD) and the molecular structure for planar *cis*-butadiene and for 1,3-cyclohexadiene and some of its allylic methyl derivatives is studied through calculation and graphical display of the rotatory strength tensor for the lowest $\pi \rightarrow \pi^*$ excitation in these systems. Also included is *cis*-butadiene in chiral structures mimicking the diene units in two of the cyclohexadiene systems. The calculations are done ab initio in the random phase approximation using an aug-cc-pVTZ atomic basis set chosen from a systematic basis set study for chiral *cis*-butadiene. For planar *cis*-butadiene this study provides the first calculation of anisotropic CD of an achiral molecule and predicts a CD intensity distribution exhibiting two numerically equal, but oppositely signed, lobes along mutually orthogonal directions perpendicular to the C_2 axis for the system. The CD intensities for the chiral molecules cyclohexadiene and its allylic derivatives exhibit two large and oppositely signed major lobes, echoing the CD of *cis*-butadiene, in addition to a nonvanishing CD intensity along the C_2 axis of the diene unit. The chirality of the ring conformation and of the arrangement of the substituents is reflected in a difference between the magnitudes of the two major lobes in the CD response and in the variation in sign and magnitude of the CD intensity along the C_2 axis. More specifically, the effects of the allylic methyl groups follow a quadrant rule and are almost additive, the effects being significantly larger for axial than for equatorial substituents. The helical twisting of the diene chromophore is of minor importance. These trends are found also for the isotropic CD, confirming earlier results. The analysis of the anisotropic CD suggests that the CD intensity along the uniaxial C_2 direction of the diene may serve as a sensitive chiral indicator for these systems.

I. Introduction

Experimental and computational studies of the relationship between structure and electronic circular dichroism (CD) of chiral molecules under isotropic conditions have a long and active history, a pivotal point of these studies being the application of CD to the determination of absolute configurations (for surveys see refs 1−5). Experimental studies of electronic CD of chiral molecules under anisotropic conditions, i.e., for oriented or partially oriented molecules, also have a relatively long but somewhat more sparse history (for surveys see refs 5 and 6), while computational studies of electronic CD of oriented molecules have appeared only quite recently.[5−8] An immediate difference between isotropic and anisotropic CD lies in the number of parameters characterizing the contributions from the individual molecules to the resulting CD and hence, conversely speaking, in the amount of structural information obtainable, at least in principle, from isotropic and anisotropic CD studies. Under isotropic conditions, the CD of a molecular excitation o $\rightarrow$ n is characterized in sign and magnitude by a single number, namely the (scalar) rotatory strength R_{on}.[9] Under anisotropic conditions, the CD contribution from the excitation o $\rightarrow$ n is characterized by the symmetric rotatory strength tensor $\mathbf{R}^s_{on}$, which contains up to six independent parameters; see refs 10−12 for discussions of the experimental determination of the rotatory strength tensor for electronic excitations, and ref 13 for a general discussion of polarized optical spectroscopy of oriented molecules. A more subtle difference between the molecular structure aspects of anisotropic and isotropic CD lies in the fact that certain classes of achiral molecules may exhibit CD under anisotropic conditions,[14,15] while the observation of isotropic CD requires the presence of chiral molecules. The existence of optical rotatory power for the nonenantiomeric crystal classes $\bar{4}2m$, m, $2mm$, and $\bar{4}$ is well established in the theory of crystal optics[16,17] and experimental evidence is also available,[18−21] while the corresponding aspect of molecular optical rotatory power apparently has been granted only a few comments in the litterature.[5,14,15] In terms of molecular point group symmetry, the condition for nonenantiomeric CD is that the molecule belongs to the point group D_{2d} or to its achiral subgroups, i.e., $C_s = C_h$, C_{2v}, and S_4, corresponding to the four optically active nonenantiomeric crystal classes.

Here we apply an ab initio computational approach[5,6] to the analysis of the relationship between enantiomeric and nonenantiomeric anisotropic electronic CD and molecular structure for systems containing the conjugated 1,3-diene chromophore. The

† Presented in part at CD '99, the seventh International Conference on Circular Dichroism. Mierki, Poland, August 1999.

* To whom correspondence should be addressed. E-mail: aaeh@rpac.ki.ku.dk.

10.1021/jp001899+ CCC: $19.00
Published on Web 11/10/2000

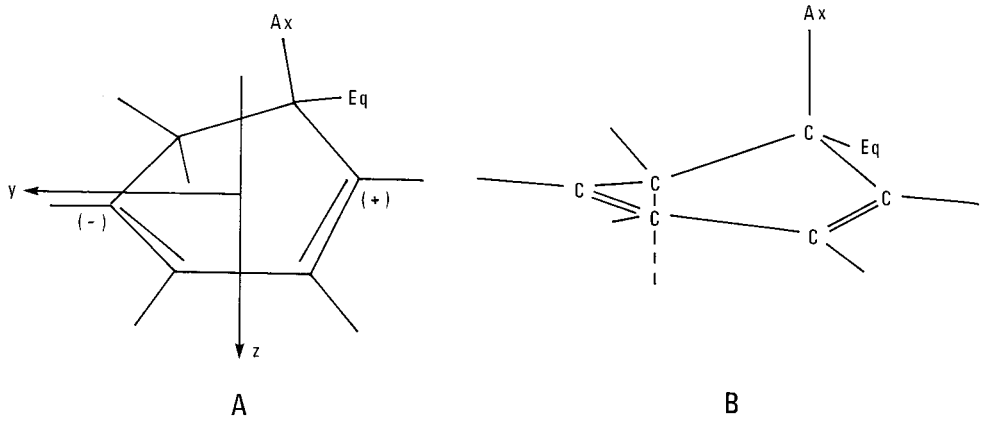

Figure 1. (A) P-helicity 1,3-cyclohexadiene. The axes indicate the Gaussian 94 standard coordinate system for this molecular structure, see section III, and (−) and (+) indicate the P (right-handed) helical twist of the chromophore. (B) P-helicity 1,3-cyclohexadiene shown in the perspective used in the displays in Figures 2 and 3.

approach is based on the random phase approximation,[4−6,22] and the systems studied here are *cis*-butadiene in an achiral planar structure, which can be expected to show nonenantiomeric CD by virtue of its C_{2v} point group symmetry, and the chiral systems 1,3-cyclohexadiene, Figure 1, and some of its mono- and disubstituted methyl derivatives. We also include the *cis*-butadiene system in chiral structures where the molecule is twisted into conformations mimicking the diene units in two of the cyclohexadiene systems. The presence of a helically twisted chromophore led to an early helicity rule[23] for the assignment of absolute configurations for cisoid 1,3-diene systems based on correlating the isotropic CD of the lowest $\pi \rightarrow \pi^*$ excitation with the sense of twist of the chromophore. Subsequently, the helicity rule was replaced by the experimental observation[24,25] that substituents in the allylic axial positions (see Figure 1) seemed to dominate over the effect of chromophore twist in determining the CD of the lowest excitation, leading to the suggestion of a quadrant rule for the perturbations from the substituents;[26] see ref 27 for a history of the study of cisoid 1,3-dienes. Ab initio calculations[27,28] provided analyses and bond decompositions of the scalar rotatory strength supporting the suggested importance of the allylic axial substituents. Recently the scalar rotatory strength of some 1,3-diene systems has been studied using a time-dependent density functional approach.[29]

For the planar *cis*-butadiene molecule, the present results and the graphical illustrations shown in sections III and IV predict strong directional CD intensity for the lowest $\pi \rightarrow \pi^*$ excitation in accord with the above anticipation of nonenantiomeric CD for this C_{2v} molecular system. For the cyclohexadiene systems the study confirms the importance of the allylic substituents for the scalar rotatory strength of these molecular systems and shows a similar influence of the allylic substituents for the rotatory strength tensor. However, the results also show a systematic variation in the rotatory strength tensor from planar butadiene through the twisted butadienes to the cyclohexadiene systems, demonstrating that characteristic and very significant features of the anisotropic CD in the chiral dienes in fact are associated with the butadiene chromophore. As discussed in section V, this analysis of the rotatory strength tensor leads to a more complete picture for the interplay between the chromophoric and extrachromophoric parts of these systems, indicating the potential of anisotropic CD for providing structural information and assisting in the assignment of absolute configurations. However, comparisons between the computed results and experimental data will not be attempted here. To our knowledge, experimental data are available only for the isotropic CD of the monosubstituted members of the series studied here,[27] while no experimental results are available for the anisotropic CD of these systems. In addition, the structural flexibility of these systems necessitates a study of the temperature-dependent equilibria, which is outside the scope of the present investigation; see refs 27 and 29 for studies of these equilibrium effects. Section VI contains our concluding remarks.

The theoretical expression for the rotatory strength tensor results from a multipolar expansion of the electromagnetic interaction between a circularly polarized light beam and a rigidly fixed molecular system.[6,10,14,30−32] In refs 6 and 31 the tensor has been obtained in forms that include an antisymmetric component, while the resulting CD intensity in fact only depends on the symmetric part of the tensor.[6,10,17,31] In section II, we present a derivation in which all references to an antisymmetric tensor components are avoided by obtaining the symmetric form of the multipolar rotatory strength tensor as the Hessian of the expansion of a fully retarded expression for anisotropic CD intensity.[32] For the illustration of the computed tensor results in section IV, we apply a graphical approach to the display of molecular tensorial response properties[33] as also outlined in section II.

II. Electronic Rotatory Strength Tensor

The CD intensity for an electronic excitation o → n in a collection of noninteracting molecules with identical spatial orientation can be written in the following, fully retarded form,[32]

$$\Delta\kappa_{no}(k) = \frac{\pi e^2 N}{\epsilon_O \hbar m^2 \omega^2}\rho_{no}(\omega)\{i\mathbf{k}\cdot[\boldsymbol{\eta}_{no}(\mathbf{k})^* \times \boldsymbol{\eta}_{no}(\mathbf{k})]\} \quad (1)$$

where N is the number of molecules per unit volume, $\rho_{no}(\omega)$ is the density of final states, i.e., a normalized line shape function, and $\mathbf{k}$ is the wavevector for a circularly polarized light beam with angular frequency ω. The quantity

$$\boldsymbol{\eta}_{no}(\mathbf{k}) = \langle n|\exp(i\mathbf{k}\cdot\mathbf{r})\mathbf{p}|o\rangle$$

is the retarded transition moment, where $\mathbf{r}$ is the electronic position vector and $\mathbf{p}$ is the corresponding linear momentum operator, suppressing the summation appropriate for many electron systems. The cross product $[\boldsymbol{\eta}_{no}(\mathbf{k})^* \times \boldsymbol{\eta}_{no}(\mathbf{k})]$ in eq 1 results in a purely imaginary vector, making the expression for $\Delta\kappa_{no}(\mathbf{k})$ purely real.

Equation 1 is valid for oriented molecular systems regardless of molecular dimensions. For molecules that are small relative to the wavelengths $\lambda = 2\pi/|k|$ in the absorption region,

expansion to second order in the wavevector k yields

$$\mathrm{i}\mathbf{k}\cdot[\boldsymbol{\eta}_{\mathrm{no}}(\mathbf{k})^* \times \boldsymbol{\eta}_{\mathrm{no}}(\mathbf{k})] = \mathrm{i}\mathbf{k}\cdot[\langle \mathrm{o}|\mathbf{p}|\mathrm{n}\rangle \times \langle \mathrm{n}|\mathbf{p}|\mathrm{o}\rangle] + \mathbf{k}\cdot[\langle \mathrm{o}|\mathbf{r}:\mathbf{p}|\mathrm{n}\rangle \times \langle \mathrm{n}|\mathbf{p}|\mathrm{o}\rangle - \langle \mathrm{o}|\mathbf{p}|\mathrm{n}\rangle \times \langle \mathrm{n}|\mathbf{p}:\mathbf{r}|\mathrm{o}\rangle]\cdot\mathbf{k} \quad (2)$$

In the presence of a static magnetic field, the wave functions are inherently complex, and the gradient term in eq 2 is then nonvanishing for electric dipole allowed transitions, accounting for the leading contributions in magnetic CD.[30] In the absence of a static magnetic field, the gradient term vanishes, and the Hessian then accounts for natural CD intensity. In this limit eq 1 becomes

$$\Delta\kappa_{\mathrm{no}}(\mathbf{k}) = \frac{4\pi\omega_{\mathrm{no}}N}{3\epsilon_{\mathrm{o}}c^2\hbar}\rho_{\mathrm{no}}(\omega)\mathbf{u}^{\dagger}\cdot\boldsymbol{R}[V]^{\mathrm{s}}_{\mathrm{no}}\cdot\mathbf{u} \quad (3)$$

Here $\omega_{\mathrm{no}} = (E_{\mathrm{n}} - E_{\mathrm{o}})/\hbar$ is the angular resonance frequency, the wavevector has been replaced by the propagation vector $\mathbf{u} = (c/\omega)\mathbf{k}$, the dagger denotes transposition, and

$$\boldsymbol{R}[V]^{\mathrm{s}}_{\mathrm{no}} = \frac{3e^2}{4m^2\omega_{\mathrm{no}}}[\langle \mathrm{o}|\mathbf{r}:\mathbf{p}|\mathrm{n}\rangle \times \langle \mathrm{n}|\mathbf{p}|\mathrm{o}\rangle - \langle \mathrm{o}|\mathbf{p}|\mathrm{n}\rangle \times \langle \mathrm{n}|\mathbf{p}:\mathbf{r}|\mathrm{o}\rangle] \quad (4)$$

is the rotatory strength tensor. The intensity determining part of eq 3, i.e.

$$R[V]_{\mathrm{no}}(\mathbf{u}) = \mathbf{u}^{\dagger}\cdot\boldsymbol{R}[V]^{\mathrm{s}}_{\mathrm{no}}\cdot\mathbf{u} \quad (5)$$

can be viewed as a directional rotatory strength. The superscript s and the qualifier [V] appearing in eqs 3−5 are discussed below.

The dyadic notation in eq 4 implies the following Cartesian elements

$$[\langle \mathrm{o}|\mathbf{r}:\mathbf{p}|\mathrm{n}\rangle \times \langle \mathrm{n}|\mathbf{p}|\mathrm{o}\rangle]_{\alpha\beta} = \Sigma_{\gamma\delta}\langle \mathrm{o}|\mathbf{r}_{\alpha}\mathbf{p}_{\gamma}|\mathrm{n}\rangle\langle \mathrm{n}|\mathbf{p}_{\delta}|\mathrm{o}\rangle\epsilon_{\gamma\delta\beta}$$

$$[\langle \mathrm{o}|\mathbf{p}|\mathrm{n}\rangle \times \langle \mathrm{n}|\mathbf{p}:\mathbf{r}|\mathrm{o}\rangle]_{\beta\alpha} = \Sigma_{\gamma\delta}\epsilon_{\beta\gamma\delta}\langle \mathrm{o}|\mathbf{p}_{\gamma}|\mathrm{n}\rangle\langle \mathrm{n}|\mathbf{p}_{\delta}\mathbf{r}_{\alpha}|\mathrm{o}\rangle = -[\langle \mathrm{o}|\mathbf{r}:\mathbf{p}|\mathrm{n}\rangle \times \langle \mathrm{n}|\mathbf{p}|\mathrm{o}\rangle]_{\alpha\beta}$$

where $\epsilon_{\alpha\beta\gamma}$ is the alternating Levi−Cevita unit tensor. The rotatory strength tensor in eq 4 is hence symmetric in the Cartesian indices, as emphasized by superscript s, while the derivations in refs 6 and 31 resulted in nonsymmetric expressions. The expression in ref 6 contains only the second term in eq 5, while the expression in ref 31 contains only the first term, both expressions scaled by a factor of ($^3/_2$) in place of the factor ($^3/_4$) in eq 5. By the same token, the electric dipole−electric quadrupole and electric dipole−magnetic dipole components in eqs 7, 8 and 14, 15 below differ from expressions in refs 6 and 31 the present expressions being manifestly symmetric. The antisymmetric components in the expressions in refs 6 and 31 are of no consequence, since both derivations result in expressions for the CD containing the symmetric sampling of the tensor represented by eq 5. However, it seems more satisfying to exploit the symmetric form of a Hessian in deriving the expression for the rotatory strength in eq 4.

Writing the dyadic transition tensors $\langle \mathrm{o}|\mathbf{r}:\mathbf{p}|\mathrm{n}\rangle$ and $\langle \mathrm{n}|\mathbf{p}:\mathbf{r}|\mathrm{o}\rangle$ as sums of symmetric and antisymmetric parts, eq 4 becomes

$$\boldsymbol{R}[V]^{\mathrm{s}}_{\mathrm{no}} = \boldsymbol{R}[V]^{\mathrm{s,q}}_{\mathrm{no}} + \boldsymbol{R}[V]^{\mathrm{s,m}}_{\mathrm{no}} \quad (6)$$

with an electric dipole−electric quadrupole component

$$\boldsymbol{R}[V]^{\mathrm{s,q}}_{\mathrm{no}} = \frac{3e^2}{8m^2\omega_{\mathrm{no}}}[\langle \mathrm{o}|\mathbf{r}:\mathbf{p} + \mathbf{p}:\mathbf{r}|\mathrm{n}\rangle \times \langle \mathrm{n}|\mathbf{p}|\mathrm{o}\rangle - \langle \mathrm{o}|\mathbf{p}|\mathrm{n}\rangle \times \langle \mathrm{n}|\mathbf{p}:\mathbf{r} + \mathbf{r}:\mathbf{p}|\mathrm{o}\rangle] \quad (7)$$

and an electric dipole−magnetic dipole tensor component

$$\boldsymbol{R}[V]^{\mathrm{s,m}}_{\mathrm{no}} = \frac{3e^2}{8m^2\omega_{\mathrm{no}}}[2\{\langle \mathrm{o}|\mathbf{p}|\mathrm{n}\rangle\cdot\langle \mathrm{n}|\mathbf{l}|\mathrm{o}\rangle\}\mathbf{1} + \langle \mathrm{o}|\mathbf{p}|\mathrm{n}\rangle:\langle \mathrm{n}|\mathbf{l}|\mathrm{o}\rangle - \langle \mathrm{o}|\mathbf{l}|\mathrm{n}\rangle:\langle \mathrm{n}|\mathbf{p}|\mathrm{o}\rangle] \quad (8)$$

where $\mathbf{l}$ is the angular momentum operator and $\mathbf{1}$ is a unit tensor. The scalar rotatory strength, which governs CD intensity under isotropic condition, is obtained as

$$R[V]_{\mathrm{no}} = \frac{1}{3}\mathrm{tr}\{\boldsymbol{R}[V]^{\mathrm{s}}_{\mathrm{no}}\} = \frac{e^2}{2m^2\omega_{\mathrm{no}}}\langle \mathrm{o}|\mathbf{p}|\mathrm{n}\rangle\cdot\langle \mathrm{n}|\mathbf{l}|\mathrm{o}\rangle \quad (9)$$

where only the electric dipole−magnetic dipole term survives since the electric dipole−electric quadrupole tensor, eq 7, is traceless. For the oscillator strength, which similarly governs ordinary electronic absorption intensity under isotropic conditions, the corresponding velocity expression is given as[4]

$$f[V]_{\mathrm{no}} = \frac{2}{3m\omega_{\mathrm{no}}\hbar}|\langle \mathrm{o}|\mathbf{p}|\mathrm{n}\rangle|^2 \quad (10)$$

The expressions in eqs 4−10 are labeled V for velocity, referring to the appearance of the momentum operator in the resulting electric dipole and quadrupole transition moments.

In addition to results obtained from eqs 6−10, we also report results obtained from equivalent intensity expressions derived by application of the hypervirial relations

$$\frac{i}{m}\langle \mathrm{o}|\mathbf{p}|\mathrm{n}\rangle = \frac{1}{\hbar}\langle \mathrm{o}|[\mathbf{r},H]|\mathrm{n}\rangle = \omega_{\mathrm{no}}\langle \mathrm{o}|\mathbf{r}|\mathrm{n}\rangle \quad (11)$$

$$\frac{i}{m}\langle \mathrm{o}|\mathbf{p}:\mathbf{r} + \mathbf{r}:\mathbf{p}|\mathrm{n}\rangle = \frac{i}{\hbar}\langle \mathrm{o}|[\mathbf{r}:\mathbf{r},H]|\mathrm{n}\rangle = \omega_{\mathrm{no}}\langle \mathrm{o}|\mathbf{r}:\mathbf{r}|\mathrm{n}\rangle \quad (12)$$

yielding the total rotatory strength tensor in the form

$$\boldsymbol{R}[L]^{\mathrm{s}}_{\mathrm{no}} = \boldsymbol{R}[L]^{\mathrm{s,q}}_{\mathrm{no}} + \boldsymbol{R}[L]^{\mathrm{s,m}}_{\mathrm{no}} \quad (13)$$

with the electric dipole − electric quadrupole component

$$\boldsymbol{R}[L]^{\mathrm{s,q}}_{\mathrm{no}} = \frac{3\omega_{\mathrm{no}}e^2}{8}[\langle \mathrm{o}|\mathbf{r}:\mathbf{r}|\mathrm{n}\rangle \times \langle \mathrm{n}|\mathbf{r}|\mathrm{o}\rangle - \langle \mathrm{p}|\mathbf{r}|\mathrm{n}\rangle \times \langle \mathrm{n}|\mathbf{r}:\mathbf{r}|\mathrm{o}\rangle] \quad (14)$$

the electric dipole − magnetic dipole component

$$\boldsymbol{R}[L]^{\mathrm{s,m}}_{\mathrm{no}} = -\frac{3ie^2}{8m}[2\{\langle \mathrm{o}|\mathbf{r}|\mathrm{n}\rangle\cdot\langle \mathrm{n}|\mathbf{l}|\mathrm{o}\rangle\}\mathbf{1} + \langle \mathrm{o}|\mathbf{r}|\mathrm{m}\rangle \times \langle \mathrm{m}|\mathbf{l}|\mathrm{o}\rangle - \langle \mathrm{o}|\mathbf{l}|\mathrm{n}\rangle:\langle \mathrm{n}|\mathbf{r}|\mathrm{o}\rangle\} \quad (15)$$

and the scalar rotatory strength

$$R[L]_{\mathrm{no}} = \frac{1}{3}\mathrm{tr}\{\boldsymbol{R}[L]^{\mathrm{s}}_{\mathrm{no}}\} = -\frac{ie^2}{2m}\langle \mathrm{o}|\mathbf{r}|\mathrm{n}\rangle\cdot\langle \mathrm{n}|\mathbf{l}|\mathrm{o}\rangle = \mathrm{Im}\{\langle \mathrm{o}|\mu_{\mathrm{e}}|\mathrm{n}\rangle\cdot\langle \mathrm{n}|\mu_{\mathrm{m}}|\mathrm{o}\rangle\} \quad (16)$$

The effect of applying eqs 11 and 12 to eqs 6−10 is to replace the momentum operator by the position operator, and eqs 13−16 are referred to as length (L) forms; μ_{e} and μ_{m} are the electric and magnetic electronic dipole operators. By the same token

the oscillator strength becomes

$$f[L]_{no} = \frac{2m\omega_{no}}{3\hbar}|\langle o|\mathbf{r}|n\rangle|^2 = \frac{2m\omega_{no}}{3e^2\hbar}|\langle o|\mu_e|n\rangle|^2 \qquad (17)$$

For later reference, the explicit expressions for two of the tensor elements in length form are

$$\{\boldsymbol{R}[L]^s_{no}\}_{zz} = -\frac{3e^2}{4m}[\langle o|\mathbf{x}|n\rangle\{i\langle n|l_x|o\rangle + m\omega_{no}\langle n|yz|o\rangle\} + \langle o|y|n\rangle\{i\langle n|l_y|o\rangle - m\omega_{no}\langle n|xz|o\rangle\}] \quad (18)$$

$$\{\boldsymbol{R}[L]^s_{no}\}_{xy} = -\frac{3e^2}{8m}[m\omega_{no}\langle 0|z|n\rangle\langle n|x^2 - y^2|o\rangle + \langle o|x|n\rangle \times \{i\langle n|l_y|o\rangle - m\omega_{no}\langle n|xz|o\rangle\} + \langle o|y|n\rangle\{i\langle n|l_x|o\rangle + m\omega_{no}\langle n|yz|o\rangle\}] \quad (19)$$

the tensor being symmetric, as discused above.

In contrast to the scalar rotatory strength, eqs 9 and 16, which contains only electric and magnetic dipole transition moments, the magnetic dipole and electric quadrupole terms appear on an equal footing in the expressions for the rotatory strength tensor, eqs 6 and 13. However, although the total rotatory strengths, eqs 6 and 13, are invariant to the (arbitrary choice of) molecular coordinate system,[6,12,30] as a consequence of the hypervirial relations in eqs 11 and 12, the relative magnitudes of the electric dipole−electric quadrupole and electric dipole−magnetic dipole contributions in eqs 6−8 and 13−15 in general depend on the choice of coordinate origin.[6,12,30] This caveat can be relaxed for some of the tensor elements in the presence of symmetry[12,34] as utilized in section V. The question of origin invariance in approximate quantum chemical computations is discussed in section III.

For discussion and illustration of the rotatory strength tensors, we use a graphical representation of the variation of the CD intensity, eq 4, relative to the molecular framework. Expressing the propagation vector u in terms of its spherical polar angles θ and ϕ relative to the molecular coordinate system the directional rotatory strength, eq 5, can be written as[5,6]

$$R_{no}(\theta,\phi) = \mathbf{u}^{\dagger}(\theta,\phi)\cdot\boldsymbol{R}^s_{no}\cdot\mathbf{u}(\theta,\phi) = R_{no} + (^1/_6)\{2R^s_{no,zz} - R^s_{no,xx} - R^s_{no,yy}\}\{3\cos^2\theta - 1\} + (^1/_2)\{R^s_{no,xx} - R^s_{no,yy}\}\sin^2\theta\cos 2\phi + R^s_{no,xy}\sin^2\theta\sin 2\phi + R^s_{no,xz}\sin 2\theta\cos\phi + R^s_{no,yz}\sin 2\theta\sin\phi \quad (20)$$

where specific reference to velocity or length versions of the tensor has been suppressed. The partial CD spectrum for the excitation o → n corresponding to a given direction of light propagation, as specified by θ and ϕ, then follows by multiplying $R_{no}(\theta,\phi)$, eq 20, by the line line shape function and the factors appearing in eq 3; see ref 5 for examples of oriented CD spectra generated by this procedure. From eq 20 it is apparent that the directional CD intensity contains an isotropic contribution governed by the rotatory strength R_{no}, eqs 9 and 16, and purely anisotropic contributions governed by the five components of the $l = 2$ (i.e., d-orbital like) real spherical harmonics scaled by the corresponding combinations of the Cartesian tensor elements. Equation 20 can be applied to the total tensor or to its electric dipole−electric quadrupole and electric dipole−magnetic dipole components, and analogous expressions can be applied to graphical illustrations of other molecular electromagnetic response tensors.[33]

TABLE 1: Hartree−Fock Groundstate Energies

system	basis	ao's	$E_{H.F}$ (au)
(C_{2v})-C_4H_6	B3LYP/6-311G**	108	−156.032167802
	aug-cc-pVTZ	322	−154.972070633
(P)-C_4H_6[1]	aug-cc-pVTZ	322	−154.966077403
(P)-C_4H_6[2]	aug-cc-pVTZ	322	−154.966066487
(P)-C_6H_8	B3LYP/6-311G**	156	−233.481329875
	cc-pVDZ	124	−231.850416661
	aug-cc-pVDZ	210	−231.858396833
	d-aug-cc-pVDZ	296	−231.859074649
	cc-pVTZ	292	−231.908831848
	aug-cc-pVTZ	460	−231.911713018
	d-aug-cc-pVTZ	628	−231.911937644
	cc-pVQZ	570	−231.924320383
	aug-cc-pVQZ	848	−231.924970550
Met[Eq]	B3LYP/6-311G**	186	−272.806563650
	aug-cc-pVTZ	552	−270.960110677
Met[Ax]	B3LYP/6-311G**	186	−272.806156159
	aug-cc-pVTZ	552	−270.959233710
DiMet[Eq]	B3LYP/6-311G**	216	−312.130114176
	aug-cc-pVTZ	644	−310.006390141
DiMet[Ax]	B3LYP/6-311G**	216	−312.130860557
	aug-cc-pVTZ	644	−310.006666693

III. Calculations and Results

The systems studied here are *cis*-butadiene in an achiral planar conformation of C_{2v} symmetry, (C_{2v})-C_4H_6, and 1,3-cyclohexadiene, (P)-C_6H_8, together with four of its allylic methyl derivatives, namely the monosubstituted (5*S*)-*equatorial*-methyl-1,3-cyclohexadiene, (P)-Met[Eq], and (5*R*)-*axial*-methyl-1,3-cyclohexadiene, (P)-Met[Ax], and the symmetrically disubstituted (5*R*,6*R*)-*diaxial*-dimethyl-1,3-cyclohexadiene, (P)-DiMet[Ax], and (5*S*,6*S*)-*diequatorial*-dimethyl-1,3-cyclohexadiene, (P)-DiMet[Eq]; see Figure 1. As indicated by the prefix in the abbreviations, the cyclic systems are all chosen to be in the P-helicity conformation where the diene chromophore is twisted in a right-handed helical form, as indicated in Figure 1. For the sake of the discussion, results for the enantiomer of (P)-DiMet[Ax], i.e., (M)-DiMet[Ax] in which the diene chromophore is twisted in a left-handed M-helicity, are included in sections IV and V. In addition, we include two distorted cisoid butadiene structures, one twisted into the chiral conformation of the diene chromophore in 1,3-cyclohexadiene, (P)-C_4H_6[1], and one twisted into the chiral conformation of the diene chromophore in (5*R*,6*R*)-*diaxial*-dimethyl-1,3-cyclohexadiene, (P)-C_4H_6[2]. Except for the distorted *cis*-butadiene systems (P)-C_4H_6[1] and (P)-C_4H_6[2] the structures are obtained by Becke3LYP/6-311G** density functional theory (DFT) optimization using the Gaussian 94 program package,[35] and the optimized DFT energies are included in Table 1. C_2 symmetry is strictly enforced for 1,3-cyclohexadiene and the two symmetric derivatives, (P)-DiMet[Ax] and (P)-DiMet[Eq]. The (P)-C_4H_6[1] and (P)-C_4H_6[2] structures are derived from the respective parent compounds.

The calculations of the rotatory strength tensor are carried out ab initio in the random phase approximation (RPA)[4,22] as described in refs 5 and 6. In the limit of a complete atomic orbital basis set, the hypervirial relations, eqs 11 and 12, are fulfilled in the RPA, and results for rotatory strengths and oscillator strengths calculated for a given excitation in velocity form, eqs 6−10, and in length form, eqs 13−17, are hence identical in this limit. By the same token, both forms of the total rotatory strength tensor, eqs 6 and 13, and of the scalar rotatory strength, eqs 9 and 16, are invariant to translations of

TABLE 2: Basis Set Dependence of RPA Results for Excitation Energy, Oscillator Strength, and Rotatory Strength[a] for the Lowest $\pi \rightarrow \pi^*$ Excitation in P-Helicity Cyclohexadiene

basis	ΔE (eV)		f	R^b	$R_{33}{}^c$	$R_{22}{}^c$	$R_{11}{}^c$	Ω^d
cc-pVDZ	5.233	V[e]	0.163	35.46	439.37	56.72	−389.74	829.11
		LAO[e]	0.157	30.34	433.41	52.51	−394.92	828.33
aug-pVDZ	5.049	V	0.151	−1.27	393.54	13.54	−410.89	804.42
		LAO	0.153	−0.68	399.30	14.82	−416.17	815.47
d-aug-pVDZ	5.049	V	0.151	−1.09	393.12	13.76	−410.15	803.29
		LAO	0.152	−0.70	398.40	14.52	−415.01	813.40
cc-pVTZ	5.127	V	0.156	21.94	423.53	41.45	−399.16	822.70
		LAO	0.153	18.36	417.63	37.75	−400.32	817.95
aug-pVTZ	5.037	V	0.151	−0.06	396.80	15.09	−412.06	808.86
		LAO	0.152	0.11	398.65	15.45	−413.78	812.43
d-aug-pVTZ	5.037	V	0.151	−0.01	396.61	15.17	−411.81	808.42
		LAO	0.152	0.12	398.02	15.39	−413.06	811.08
cc-pVQZ	5.086	V	0.153	13.31	413.52	31.24	−404.85	818.37
		LAO	0.152	11.70	410.86	29.54	−405.30	816.16
aug-pVQZ	5.036	V	0.152	0.20	397.60	15.42	−412.43	810.03
		LAO	0.152	0.20	398.08	15.55	−413.03	811.10

[a] In units of 10^{-40} cgs. [b] Isotropic rotatory strength. [c] Principal Axes Values of the rotatory strength tensor. [d] Span, $\Omega = R_{33} - R_{11}$. [e] Intensity formalism: V = velocity, LAO = London atomic orbitals. See text for the oscillator strengths labeled LAO.

the origin of the molecular coordinate system in this limit.[6] The origin dependence of the separation of the rotatory strength tensor into electric dipole−electric quadrupole and electric dipole−magnetic dipole contributions, referred to in section II, is a fundamental aspect of this separation and is unrelated to questions of computational method and quality.

In finite basis set RPA calculations, the computed length and velocity results become different, and translational invariance is no longer guaranteed for the two formulations. With so-called conventional (i.e., perturbation independent) basis sets, results from the length expressions in eqs 13 and 16 depend on the origin, while results from the velocity expressions in eqs 6 and 9 are origin invariant.[6,36] With magnetic field dependent basis sets, the so-called London atomic orbitals (LAO's), the situation is reversed, and results from the length expressions, eqs 13 and 16, become origin invariant, while results from the velocity expressions, eqs 6 and 9, depend on the origin.[37] The presence of symmetry may lead to additional origin invariances.[34,38] Note that the magnetic field dependence in an LAO basis only affects the magnetic dipole transition moment.[37] The LAO results for the electric dipole−electric quadrupole component, eqs 7 and 14, and for the oscillator strength, eqs 10 and 17, are therefore identical to results obtained with the corresponding conventional basis.

The atomic basis set used in the present calculations is chosen from a study of RPA results for the lowest $\pi \rightarrow \pi^*$ excitation of the P-helicity 1,3-cyclohexadiene system, (P)-C_6H_8, using the basis sets cc-pVDZ, cc-pVTZ, cc-pVQZ plus augmented versions of these sets and double-augmented versions of cc-pVDZ and cc-pVTZ.[39−41] The prerequisite Hartree−Fock calculations, and the RPA calculations are performed with the Dalton program package.[42] The Hartree−Fock groundstate energies and the number of contracted basis functions for the various basis sets are included in Table 1, and the RPA results are shown in Table 2. In addition to the transition energies, Table 2 displays the oscillator strengths, the scalar rotatory strengths, the principal values of the total tensors, using the index convention $R_{33} > R_{22} > R_{11}$, and the span, $\Omega = R_{33} - R_{11}$. The oscillator and rotatory strength results are calculated in the velocity formulation, eqs 6−10, using conventional versions of these basis sets, and in the length formulation, eqs 13−17, using London atomic orbital versions of the basis sets. As mentioned above, the oscillator strength results reported for London atomic orbitals are identical to length results resulting from the corresponding conventional basis. The principal values are found by diagonalization of the corresponding tensors, and represent the CD intensities along the principal axes, while the span measures the total variation of the CD intensity for the excitation. See, e.g., ref 33 for these tensor concepts.

TABLE 3: RPA Results[a] for the Rotatory Strength Tensors[b] for the Lowest $\pi \rightarrow \pi^*$ Excitation in Planar Butadiene and in P-Helicity Butadiene, Cyclohexadiene, and Its Methyl Derivatives

	R(V)			**R**(LAO)		
(C_{2v})-C_4H_6	0.000			0.000		
	499.825	0.000		501.630	0.000	
	0.000	0.000	0.000	0.000	0.000	0.000
(P)-C_4H_6[1]	0.490			0.962		
	429.950	18.814		431.628	18.531	
	0.000	0.000	−12.294	0.000	0.000	−12.902
(P)-C_4H_6[2]	427.447			429.196		
	81.441	−416.025		81.380	−417.679	
	0.000	0.000	−16.013	0.000	0.000	−16.565
(P)-C_6H_8	−86.063			−86.365		
	396.751	70.804		398.498	71.243	
	0.000	0.000	15.094	0.000	0.000	15.448
Met[Eq]	21.420			21.703		
	14.267	5.473		14.246	5.676	
	234.632	325.794	−46.126	235.509	327.246	−46.277
DiMet[Eq]	63.554			63.794		
	400.629	−93.644		402.236	−93.936	
	0.000	0.000	−11.497	0.000	0.000	−11.257
Met[Ax]	−39.649			−40.083		
	139.296	41.205		139.853	41.224	
	189.939	−310.132	142.829	190.677	−311.296	143.419
DiMet[Ax]	397.178			398.446		
	165.598	−310.478		166.067	−311.841	
	0.000	0.000	203.239	0.000	0.000	203.607

[a] Basis set: aug-cc-pVTZ. [b] In units of 10^{-40} cgs.

Table 2 shows that the RPA results obtained with the augmented basis sets appear to be close to a convergence limit with good, increasing to excellent, agreement between results obtained from the two equivalent intensity expressions, while only minor additional improvements are obtained with the double-augmented sets. On the other hand, even the largest nonaugmented basis set, cc-pVQZ, produces results that are quite far from the results with the augmented sets. For the tensorial characteristics, the table shows a consistent pattern of large oppositely signed R_{11} and R_{33} principal values, the effect of basis set augmentation being a moderate reduction of the span of the principal values. From these results the aug-cc-pVTZ set of atomic functions seem an adequate compromise between accuracy and economy, and are deployed in the calculations for the full set of molecular systems studied here. The aug-cc-pVTZ Hartree−Fock groundstate energies for these systems are included in Table 1.

Table 3 displays the RPA results for the rotatory strength tensors of the lowest $\pi \rightarrow \pi^*$ excitation in the various molecular systems obtained using the Dalton program package[42] with the aug-cc-pVTZ atomic basis set as argued above; the agreement between the results for the two intensity formulations is seen to be quite satisfactory. The table shows the lower half of these symmetric tensors, expressed in the Gaussian 94 Cartesian standard coordinate systems.[35] These standard coordinate systems reflect molecular point group symmetries, and the structures of the tensors in Table 3 therefore follow from point group selection rules, as discussed further in section V. However, in the standard systems the axes that do no not coincide with symmetry axes are rotated from molecule to molecule in a way

TABLE 4: RPA Results[a] for Excitation Energies, Oscillator Strengths, and Rotatory Strengths[b] for the Lowest $\pi \rightarrow \pi^*$ Excitation in Planar Butadiene and in P-Helicity Butadiene, Cyclohexadiene, and Its Methyl Derivatives

	DiH[c] (deg)	ΔE (eV)		f	R^d	$R_{33}{}^e$	$R_{22}{}^e$	$R_{11}{}^e$	Ω^f
(C_{2v})-C_4H_6	0.0	5.283	V[g]	0.316	0.00	499.82	0.00	−499.82	999.64
			LAO[g]	0.317	0.00	501.63	0.00	−501.63	1003.26
(P)-C_4H_6[1]	14.4	5.040	V	0.216	2.34	439.70	−12.29	−420.40	860.09
			LAO	0.217	2.20	441.46	−12.90	−421.97	863.43
(P)-C_4H_6[2]	11.7	5.009	V	0.216	−1.53	435.24	−16.01	−423.82	859.05
			LAO	0.217	−1.68	436.93	−16.57	−425.43	862.37
(P)-C_6H_8	14.4	5.037	V	0.151	−0.06	396.80	15.09	−412.06	808.60
			LAO	0.152	0.11	398.65	15.45	−413.78	812.43
Met[Eq]	14.4	5.004	V	0.144	−6.41	392.40	2.40	−414.04	806.44
			LAO	0.145	−6.30	394.13	2.68	−415.71	809.84
DiMet[Eq]	13.6	4.966	V	0.139	−13.86	393.22	−11.50	−423.31	816.53
			LAO	0.139	−13.80	394.82	−11.26	−424.96	819.79
Met[Ax]	12.9	5.036	V	0.144	48.13	414.30	108.89	−378.80	793.10
			LAO	0.144	48.19	415.83	109.11	−380.39	796.22
DiMet[Ax]	11.7	5.046	V	0.140	96.66	434.01	203.24	−347.31	781.32
			LAO	0.141	96.75	435.35	203.61	−348.75	784.10

[a] Basis set: aug-cc-pVTZ. [b] In units of 10^{-40} cgs. [c] Dihedral angle of butadiene fragment. [d] Isotropic rotatory strength. [e] Principal axes values of the rotatory strength tensor. [f] Span, $\Omega = R_{33} - R_{11}$. [g] Intensity formalism: V = velocity, LAO = London atomic orbitals. See text for the oscillator strengths labeled LAO.

that makes it rather difficult directly to analyze the trends and changes in magnitudes in the tensors. The changes in the resulting CD intensities represented in terms of the principal value intensities are apparent in Table 4, while the actual anisotropic CD intensity distributions relative to the molecular frameworks are shown in the graphical representations in section IV. Here we note only that the traceless rotatory strength tensor for the achiral butadiene system, (C_{2v})-C_4H_6, in fact contains a large nonzero off-diagonal tensor element.

Table 4 summarizes the overall results in parallel to the presentation in Table 2. In addition to entries discussed in the context of Table 2, Table 4 includes the dihedral angle for the diene chromophore in the various structures, the positive values corresponding to P-helicity conformations. It is clear from Table 4 that the excitation energy of the $\pi \rightarrow \pi^*$ transition is almost completely governed by the distorted diene unit. The total variation in the energy is less than ± 0.05 eV going from the twisted (P)-C_4H_6 butadiene systems through the series of cyclohexadiene systems. At the same time, the variations in the computed rotatory strengths are not in any way correlated with the very small variations in the chromophore twist as measured by the dihedral angle. For the scalar rotatory strengths, the resulting values for (P)-C_4H_6[1], (P)-C_4H_6[2], and (P)-C_6H_8 are small, and the rotatory strength for (C_{2v})-C_4H_6 of course vanishes identically. In the substituted cyclohexadiene sequence, substituents in equatorial positions generate essentially additive negative values for the scalar rotatory strength, while substituents in axial positions generate essentially additive positive values, the effect of axial substitution being significantly larger than the effect of equatorial substitution. These findings are in qualitative agreement with our earlier results[27,28] and with the quadrant rule proposed in ref 26, both with regard to the overruling importance of the allylic substituents relative to the importance of the twisted butadiene chromophore for the scalar rotatory strength and with regard to the signs and relative magnitudes of the effects of axial and equatorial substituents. However, the present results differ numerically quite markedly from our earlier results primarily because of basis set improvements relative to the STO-4G basis set used in ref 27 and the double-ζ quality basis set used in ref 28.

For the tensorial results in Table 4, the nonvanishing rotatory strength tensor listed in Table 3 for (C_{2v})-C_4H_6 results in the two large, numerically equal but oppositely signed, R_{11} and R_{33} principal values and a strictly vanishing R_{22} principal value. The pattern of large and oppositely signed R_{11} and R_{33} principal values was noted for (P)-C_6H_8 in Table 2, and is found for all the systems in Table 4. For the cyclohexadiene systems, the variations of the scalar rotatory strengths noted above are found also as general trends for the tensors. Equatorial substituents reduce the magnitude of the positive R_{33} principal values, make the negative R_{11} principal values more negative, and reduce the positive R_{22} for the unsubstituted system to a negative value for DiMet[EQ]. Conversely, axial substituents increase the positive R_{22} and R_{33} principal value and make R_{11} significant less negative. As with the scalar rotatory strengths, the effects of the substituents tend to be additive. The direction of the principal axes corresponding to the various principal values are not listed, but are immediately apparent in the graphical illustrations shown in the next section, see also the discussion in section V.

IV. Graphical Representations

The anisotropic CD intensity distributions predicted from the computed rotatory strengths tensors in Table 3 by use of eq 20 are shown in Figure 2 for C_{2v} *cis*-butadiene and its twisted variants (P)-C_4H_6[1] and (P)-C_4H_6[2], and in Figure 3 for the 1,3-cyclohexadiene systems including the M-helicity conformer of diaxially substituted 1,3-cyclohexadiene, (M)-DiMet[Ax]. The latter structure is generated from the (P)-DiMet[Ax] structure by inversion of all Cartesian coordinates, and the rotatory strength tensor is generated by changing all signs in the (P)-DiMet[Ax] tensor (Table 3). The structures in the figures are all oriented as shown in Figure 1 B, except that (M)-DiMet-[Ax] is rotated into a mirror image position of (P)-DiMet[Ax]. The individual CD response graphs in Figures 2 and 3 are centered at the central C−C bond in the diene chromophore in the various molecular structures, and the distance along a given direction from the center of a graph to the surface provides the magnitude of the CD for a light beam propagating along that direction, the sign of the CD being positive (negative) for blue (red) contours of the surface. The surfaces therefore show the variation in the CD intensity for the lowest $\pi \rightarrow \pi^*$ excitation in these systems as the impingent circularly polarized light beam samples all directions relative to the space-fixed molecular structure. The scale chosen for the graphs, relative to the scale used for the molecular structure, is such that a distance of 1 Å corresponds to a value of 250×10^{-40} cgs for the directional rotatory strength $R_{no}(\theta,\phi)$, eq 20. The graphs are generated by

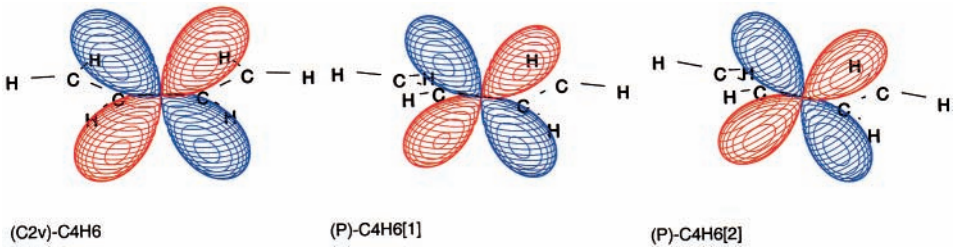

Figure 2. Response graphs for the CD intensity distribution for the lowest $\pi \rightarrow \pi^*$ excitation in C_{2v} *cis*-butadiene and its twisted variants (P)-C_4H_6[1] and (P)-C_4H_6[2], see text. Scale: 1 Å $\approx 250 \times 10^{-40}$ cgs.

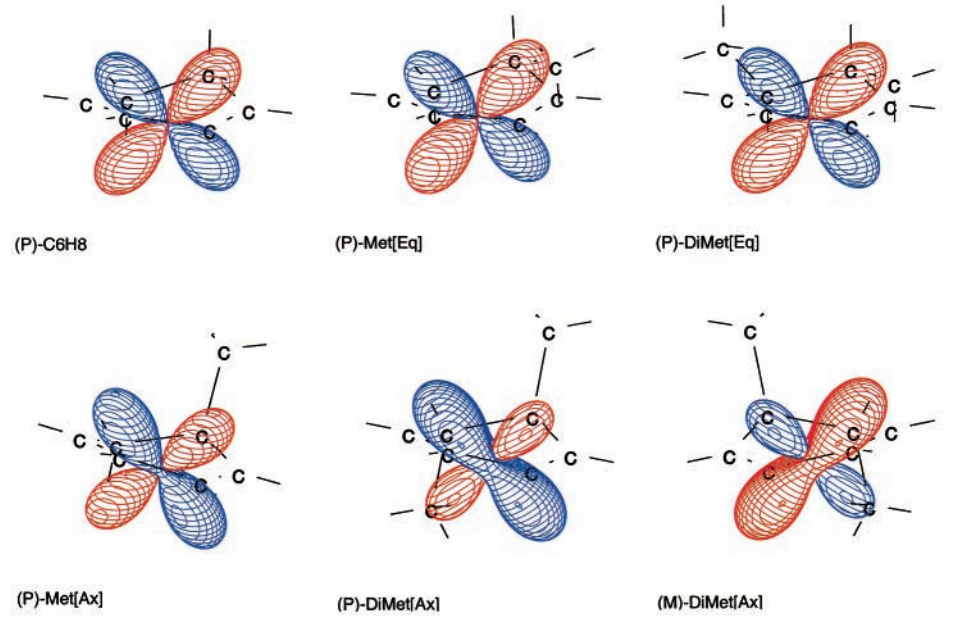

Figure 3. Response graphs for the CD intensity distribution for the lowest $\pi \rightarrow \pi^*$ excitation in the 1,3-cyclohexadiene systems including the M-helicity conformer of diaxially substituted 1,3-cyclohexadiene, (M)-DiMet[Ax], see text. Scale: 1 Å $\approx 250 \times 10^{-40}$ cgs.

the graphics module in the RPAC program package[43] using the computed rotatory strength tensors obtained in the length form with the LAO version of the aug-cc-pVTZ atomic orbital basis, Table 4.

In the graphs, the principal values listed in Table 4 are hence found as the distance from the centers to the extremum points of the surfaces, applying the scale factor given above, and the directions to the extremum points represent the directions of the corresponding principal axes. In this way, the large and oppositely signed R_{11} and R_{33} principal values and axes are easily identified in all cases, while the R_{22} principal values only become visible for the two axially substituted derivatives at the resolution imposed by the scale factor used in the present graphs. However, the axes corresponding to the R_{22} principal values evidently lie along the C_2 axes of the symmetric molecules and along the corresponding directions in the two monomethylated nonsymmetric derivatives. In terms of the various contributions in eq 20, the shape of the graphs show a strong dominance of the anisotropic contributions governed by the $l = 2$ spherical harmonics over the isotropic contribution. Since the scalar rotatory strength vanishes identically for (C_{2v})-C_4H_6, the intensity graph for this system is an uncontaminated $l = 2$ (d_{xy} type) spherical harmonic.

The graphs reveal a similarity in the CD intensity distributions relative to the molecular structures that is not easily anticipated from the tensors listed in Table 3, because of the coordinate rotations discussed in section III. In fact, the directions and signs of the two dominating lobes in all cases strongly echo the anisotropic CD intensity distribution in the planar achiral (C_{2v})-C_4H_6 system. From the graphs the negative and positive scalar rotatory strengths developed with, respectively, equatorial and axial substitutions are seen to arise from a combination of increased unbalance of the positive and negative intensity lobes and changes in the R_{22} principal value, essentially retaining the overall directional properties of the CD response. The persistence of the sign distribution in the CD intensity lobes is emphasized by Figure 3e,f, which juxtapose the CD intensity in (P)-DiMet[Ax] and in its enantiomer (M)-DiMet[Ax]. Here the reflection from one enantiomeric structure to the other is followed by reflection and sign inversion of the CD response, in accord with the pseudotensor quality of the rotatory strength tensor, and the accompagnying sign changes in the scalar rotatory strength and in the principal values are easily visualized in the two graphs. However at the same time, the sign distribution of the two major lobes relative to the butadiene chromophoric group is retained from the C_{2v} butadiene graph in both enatiomers.

V. Discussion and Structural Correlations

Anisotropic CD for Planar *cis*-Butadiene. The appearance of anisotropic CD in this achiral system can be anticipated, following Barron,[14] by realizing that the diene unit appears as a left-handed helix for light propagating along the axis corresponding to the negative principal value R_{11}, i.e., the axis of the red lobes of Figure 2a, and as a right-handed helix for light propagating along the axis corresponding to the positive principal value R_{33}, i.e., the axis of the blue lobes of Figure 2a. However, this change in the apparent helicity from one principal

axis direction to the other of course only predicts a sign change in the anisotropic CD distribution; the actual signs and magnitudes depend on the particular excitation.

Alternatively, the anisotropic CD of butadiene can be discussed in terms of the selection rules for the C_{2v} point group (see, e.g., ref 44), as applied to the expressions for the elements of the rotatory strength tensor, eqs 14, 15 and 18, 19. It follows immediately that all tensor elements vanish identically for the electric dipole forbidden A_2 excitations, while the symmetry allowed transition matrix elements for A_1, B_1, and B_2 excitations predict a nonvanishing value for, respectively, the first, second, and third term in the $xy = yx$ off-diagonal tensor element, eq 19, using the coordinate convention in ref 44. All other tensor elements vanish identically; cfr. the gyration tensor for the crystal class 2 mm listed in ref 16. The present choice of axes, Figure 1, makes the lowest $\pi \rightarrow \pi^*$ excitation transform as B_2, accounting for the nonvanishing $[\boldsymbol{R}(L)^{s}_{no}]_{xy}$ tensor element reported in Table 3. As shown in Table 4 and Figure 2, the resulting maximum values for the directional CD intensity are large, about $\pm 500 \times 10^{-40}$ cgs.

Anisotropic CD for the Cyclohexadiene Systems. For the nonsymmetric monosubstituted (P)-Met[Eq] and (P)-Met[Ax] molecular systems, no point group selection rules can be invoked, and all elements of the total rotatory strength tensor for the $\pi \rightarrow \pi^*$ excitation listed in Table 3 are nonvanishing. On the other hand, for the C_2 point group of (P)-C_4H_6[1], (P)-C_4H_6[2], (P)-C_6H_8, and the two symmetric dimethyl-substituted species, (P)-DiMet[Eq] and (P)-DiMet[Ax] application of the appropriate selection rules[44] for the tensor elements in eqs 14, 15 and 18, 19, generates the following generic structure for the total rotatory strength tensor

$$\begin{Bmatrix} xx & & \\ yx & \text{yy} & \\ 0 & 0 & zz \end{Bmatrix} \tag{21}$$

in coordinate systems where the *z*-axis coincides with the C_2 axis. The structure shown in eq 21 applies to both A and B excitations in systems of C_2 point group symmetry; cfr. the gyration tensor for the crystal class 2 listed in ref 16. For the present set of C_2 systems, the lowest $\pi \rightarrow \pi^*$ excitation transforms as the B representation, and since the Gaussian 94 standard coordinate systems[35] identify the *z*-axis with the C_2 axis, the corresponding tensors in Table 3 all exhibit the structure shown in eq 21.

The origin dependence discussed in section 2 for the separation of the total rotatory strength tensor into multipolar components, eqs 6−8 and 13−15, implies that the generic structure shown in eq 21 does not necessarily apply to the multipolar components of the tensor, since an element that is strictly vanishing for symmetry reason for the total tensor may become nonvanishing, but of course with numerically equal and oppositely signed values, in the two multipolar tensor components. The origin dependence also implies that analysis of the elements of the total tensor into multipolar components for the purpose of structure correlations is not meaningful in general. However, in the uniaxial chiral point groups C_n, symmetry not only forces one of the principal axes of the total rotatory strength tensor to coincide with the axis of rotation, for the present C_2 systems leading to $R_{22} = R_{zz}$. The uniaxial symmetry also ensures that the multipolar separation of this particular tensor element in fact is origin invariant and hence physically meaningful,[12,34] and Table 5 shows the resulting decomposition of the computed $R_{22} = R_{zz}$ tensor elements for the C_2 systems. Despite variations in the relative magnitudes, both multipolar contributions are clearly important for all members of this series of molecules.

TABLE 5: RPA Results[a] for the *zz* Element of the Rotatory Strength Tensor[b,c] for the Lowest $\pi \rightarrow \pi^*$ Excitation in P-Helicity Butadiene, Cyclohexadiene, and Its Symmetric Dimethyl Derivatives

		R^{q}_{zz}	R^{m}_{zz}	R^{s}_{zz}
(P)-C_4H_6[1]	V[d]	−15.79	3.49	−12.29
	LAO[d]	−16.21	3.30	−12.90
(P)-C_4H_6[2]	V[d]	−13.72	−2.31	−16.01
	LAO[d]	−14.05	−2.55	−16.57
(P)-C_6H_8	V	15.18	−0.09	15.09
	LAO	15.27	0.14	15.45
DiMet[Eq]	V	9.29	−20.79	−11.50
	LAO	9.43	−20.22	−11.26
DiMet[Ax]	V	58.27	144.97	203.24
	LAO	58.51	145.11	203.61

[a] Basis set: aug-cc-pVTZ. [b] In units of 10^{-40} cgs. [c] See eqs 6−8 and 13−16 for the separation of the tensor elements into the *q* and *m* contibutions. [d] Intensity formalism: V = velocity, LAO = London atomic orbitals.

Structural Information from the Rotatory Strength Tensor. It follows from the above discussion and from Figures 2 and 3, that the strong $l = 2$ (d_{xy} type) spherical harmonic contribution persisting in the CD response of all members of the present family of molecular systems provides an essentially achiral piece of structure information, viz. the presence of a chromophore of nearly C_{2v} point group symmetry. For cyclohexadiene and its derivatives the chirality of the ring conformation and of the arrangement of the substituents is reflected in the unbalance of the major lobes in the CD response, quantified in the R_{11} and R_{33} principal values for the rotatory strength tensor, and in the variation in sign and magnitude of the R_{22} principal value. However, assuming the corresponding CD measurement could be done, extraction of the chiral information represented by the R_{11} and R_{33} principal values for the CD of these systems would not be so easy, since this information is contained in intensity increase or decrease relative to the intensity distribution for the achiral planar butadiene system under retention of the signs of the CD response along the directions of the principal lobes, as illustrated by the response graphs for (P)-DiMet[Ax] and its enantiomer (M)-DiMet[Ax] in Figure 3. On the other hand, the R_{22} principal value acts as a genuine chiral indicator. It is identically zero in the achiral C_{2v} parent system and shows large and structurally characteristic variations in sign and magnitude for this series of molecular systems. We note in particular that the significant difference in R_{22} values for the two model systems (P)-C_4H_6[1] and (P)-C_4H_6-[2] on one hand, and the (P)-C_6H_8 full ring system on the other, reflects the influence of the C_5-C_6 backbone bond, in contrast to the situation for the scalar rotatory strengths where the differences between the model systems and the full ring system are marginal. In addition, although the effects of axial and equatorial allylic substitutions largely follow a quadrant rule, as is the case also for the scalar rotatory strengths, Table 4 and ref 26, the differences between the effect of axial and equatorial substitutions are emphasized significantly by the R_{22} values relative to the scalar rotatory strengths. From an experimental point of view, the fact that the principal axes corresponding to the R_{22} principal value coincides with the uniaxial direction for the symmetric species, and lies along a structurally closely related direction for the two nonsymmetric species, implies (at least in principle) that this principal value should be amenable to experimental determination,[12] and the characteristic structural correlations discussed above hence suggests that the R_{22} value

potentially might serve as a sensitive chirality measure for these systems. From a theoretical point of view, it follows from Table 5 that any modeling of the structural correlations for the R_{22} value must take electric dipole−electric quadrupole and electric dipole−magnetic dipole terms into account on an equal footing, in contrast to conventional static perturbation based sector rules for the electric dipole−magnetic dipole expression for the scalar rotatory strength.[26,45,46]

VI. Summary and Concluding Remarks

We have presented an ab initio computational study within the random phase approximation (RPA) of the anisotropic circular dichroism (CD) of *cis*-butadiene and of cyclohexadiene and some of its methyl derivatives. For the planar *cis*-butadiene system of C_{2v} molecular point group symmetry, the present study represents the first calculations of the anisotropic circular dichroism (CD) intensity of an achiral, or nonenantiomeric, molecular system, and the calculations predict very large, numerically equal but oppositely signed, CD intensities along two of the mutually orthogonal principal axes of the rotatory strength tensor for the lowest $\pi \rightarrow \pi^*$ excitation of this system. We show also how anisotropic CD can be anticipated for this system by applying point group selection rules to the elements of the rotatory strength tensor that governs the anisotropic CD intensity.

As outlined in the Introduction, the earliest approach to structural correlations for the isotropic CD of the lowest $\pi \rightarrow \pi^*$ excitation in the chiral molecular systems cyclohexadiene and its methyl-substituted derivatives proposed assignments of the absolute configuration based on the helicity of the inherently chiral twisted diene chromophore.[23] Later experimental and theoretical studies[24−28] led to a picture according to which contributions to the resulting isotropic CD intensity relating to the inherent chirality of the twisted diene chromophore could be discarded in favor of contributions relating to the arrangement of allylic substituents. The picture emerging from the present study of the anisotropic CD of these systems again places the diene chromophore in a central role in the sense that the presence of a chromophore of C_{2v} or nearly C_{2v} symmetry imposes a strong $l = 2$ (d_{xy} type) spherical harmonic contribution on the resulting CD intensity distribution, while the presence of allylic substituents is revealed by major chiral modifications of the diene signal with only minor modifications caused by the twist of the diene unit. At the same time, since there is no isotropic contribution from the $l = 2$ part of the anisotropic CD, the present picture recovers the dominating influence of the allylic substituents in the isotropic CD. The present analysis also suggests that the R_{22} principal value of the rotatory strength tensor, which is observed as the CD intensity along the C_2 axis of the diene chromophore, may serve as a sensitive chiral indicator for these systems.

We note finally that we the graphical approach described and illustrated in section III for the rotatory strength tensor provides a powerful tool for the analysis and structural interpretation of the computed numerical results for a range of molecular electromagnetic response tensors.[33]

Acknowledgment. This work has been supported by The Danish Research Councils through Grants 9600856 and 9701136.

References and Notes

(1) Kuhn, W. *Annu. Revs. Phys. Chem.* **1958**, *9*, 417.
(2) Caldwell, D. J.; Eyring, H. *Annu. Revs. Phys. Chem.* **1964**, *15*, 281.
(3) Deutsche, C. W.; Lightner, D. A.; Woody, R. W.; Moscowitz, A. *Annu. Revs. Phys Chem.* **1969**, *20*, 407.
(4) Hansen, Aa. E.; Bouman, T. D. *Adv. Chem. Phys.* **1980**, *44*, 546.
(5) Hansen, Aa. E.; Bak, K. L. *Enantiomer* **1999**, *4*, 455.
(6) Pedersen, T. B.; Hansen, Aa. E. *Chem. Phys. Lett.* **1995**, *246*, 1.
(7) Pedersen, T. B.; Koch, H.; Ruud, K. *J. Chem. Phys.* **1999**, *110*, 2883.
(8) Pedersen, T. B.; Koch, H. *J. Chem. Phys.* **2000**, *112*, 2139.
(9) Moscowitz, A. *Adv. Chem. Phys.* **1962**, *4*, 67.
(10) Kuball, H.-G.; Karstens, T.; Schönhofer, A. *Chem. Phys.* **1976**, *12*, 1.
(11) Kuball, H.-G.; Altschuh, J.; Schönhofer, A. *Chem. Phys.* **1979**, *12*, 67.
(12) Kuball, H.-G.; Sieber, G.; Neubrech, S.; Schultheis, B.; Schönhofer, A. *Chem. Phys.* **1993**, *169*, 335.
(13) Schellman, J. A.; Jensen, H. P. *Chem. Rev.* **1987**, *87*, 1359.
(14) Barron, L. D. *Molecular Light Scattering and Optical Activity*; Cambridge University Press: Cambridge, U.K., 1982.
(15) Osipov, M. A.; Pickup, B. T.; Dunmur, D. A. *Mol. Phys.* **1995**, *84*, 1193.
(16) Nye, J. F. *Physical Properties of Crystals*; Oxford University Press: Oxford, U.K., 1957.
(17) Ramachandran, G. N.; Ramaseshan, S.; In *Handbuch der Physik*; Flügge, S., Ed.; Springer-Verlag: Berlin, 1961; Band XXV/1.
(18) Hobden, M. V. *Nature* **1967**, *216*, 678.
(19) Hobden, M. V. *Acta Crystallogr.* **1968**, *A24*, 676.
(20) Hobden, M. V. *Acta Crystallogr.* **1969**, *A25*, 633.
(21) Chern, M.-J.; Phillips, R. A. *J. Opt. Soc. Am.* **1970**, *60*, 1230.
(22) Oddershede, J.; Jørgensen, P.; Yeager, D. L. *Comput. Phys. Rept.* **1984**, *2*, 33.
(23) Moscowitz, A.; Charney, E.; Weiss, U.; Ziffer, H. *J. Am. Chem. Soc.* **1961**, *83*, 4661.
(24) Burgstahler, A. W.; Barkhurst, R. C. *J. Am. Chem. Soc.* **1970**, *92*, 7601.
(25) Burgstahler, A. W.; Weigel, L. O.; Gawronski, J. K. *J. Am. Chem. Soc.* **1976**, *98*, 3015.
(26) Moriarty, R. M.; Paaren, H. E.; Weiss, U.; Whalley, W. B. *J. Am. Chem. Soc.* **1979**, *101*, 6804.
(27) Lightner, D. A.; Bouman, T. D.; Gawronski, J. K.; Gawronska, K.; Chappuis, J. L.; Crist B. V.; Hansen, Aa. E. *J. Am. Chem. Soc.* **1981**, *103*, 5314.
(28) Hansen, Aa. E.; Bouman, T. D.; In *Proc. of the 2nd International Conference on Circular Dichroism*; Kajtar, M., Ed. L. Eötvös University: Budapest, Hungary, 1987.
(29) Cheeseman, J. R.; Frisch, M. J.; Devlin, F. J.; Stephens, P. J. 7th International Conference on Circular Dichroism, Mierki, Poland, 1999.
(30) Stephens, P. J. *J. Chem. Phys.* **1970**, *52*, 3489.
(31) Snir, J.; Schellman, J. *J. Phys. Chem.* **1973**, *77*, 1653.
(32) Hansen, Aa. E.; Avery, J. S. *Chem. Phys. Lett.* **1972**, *13*, 396.
(33) Hansen, Aa. E.; Mikkelsen, K. V.; Bak, K. L. *Magn. Reson. Rev.* **1997**, *17*, 133.
(34) Hansen, Aa. E. To be published.
(35) Frisch, M. J.; Trucks, G. W.; Schlegel, H. B.; Gill, P. M. W.; Johnson, B. G.; Robb, M. A.; Cheeseman, J. R.; Keith, T.; Petersson, G. A.; Montgomery, J. A.; Raghavachari, K.; Al-Laham, M. A.; Zakrzewski, V. G.; Ortiz, J. V.; Foresman, J. B.; Cioslowski, J.; Stefanov, B. B.; Nanayakkara, A.; Challacombe, M.; Peng, C. Y.; Ayala, P. Y.; Chen, W.; Wong, M. W.; Andres, J. L.; Replogle, E. S.; Gomperts, R.; Martin, R. L.; Fox, D. J.; Binkley, J. S.; Defrees, D. J.; Baker, J.; Stewart, J. P.; Head-Gordon, M.; Gonzalez, C.; Pople, J. A. *Gaussian 94*, Revision D.3; Gaussian, Inc.: Pittsburgh, PA, 1995.
(36) Moscowitz, A. In *Modern Quantum Theory*; Sinanoglu, O., Ed.; Academic Press: New York, 1965; Vol. 3.
(37) Bak, K. L.; Hansen, Aa. E.; Ruud, K.; Helgaker, T.; Olsen, J.; Jørgensen, P. *Theor. Chim. Acta* **1995**, *90*, 441.
(38) Hansen, Aa. E. *Mol. Phys.* **1967**, *13*, 425.
(39) Dunning, T. H., Jr. *J. Chem. Phys.* **1989**, *90*, 1007.
(40) Kendall, R. A.; Dunning, T. H., Jr.; Harrison, R. J. *J. Chem. Phys.* **1992**, *96*, 6796.
(41) Woon, D. E.; Dunning, T. H., Jr. *J. Chem. Phys.* **1994**, *96*, 6796.
(42) Helgaker, T.; Jensen, H. J. Aa.; Jørgensen, P.; Koch, H.; Olsen, J.; Aagren, H.; Andersen, T.; Bak, K. L.; Bakken, V.; Christiansen, O.; Dahle, P.; Dalskov, E. K.; Enevoldsen, T.; Halkier, A.; Heiberg, H.; Jonsson, D.; Kirpekar, S.; Kobayashi, R.; de Meras, A. S.; Mikkelsen, K. V.; Norman, P.; Packer, M. J.; Ruud, K.; Saue, T.; Taylor, P. R.; Vahtras, O. *DALTON, an Electronic Structure Program*, Version 1.0; 1996. www.kjemi.uio.no/software/dalton/dalton.html
(43) Bouman, T. B.; Hansen, Aa. E.; Pedersen, T. B.; Bak K. L.; Kirby, R. A. *Program* RPAC, Molecular Properties Package, Version 11.0; University of Copenhagen, Denmark, 1995.
(44) Atkins, P. W.; Childs, M. S.; Phillips, C. S. G. *Tables for Group Theory*; Oxford University Press: Oxford, U.K., 1970.
(45) Moffitt, W.; Woodward, R. B.; Moscowitz, A.; Klyne, W.; Djerassi, C. *J. Am. Chem. Soc.* **1961**, *83*, 4013.
(46) Schellman, J. A. *J. Chem. Phys.* **1966**, *44*, 55.